Ain Shams Engineering Journal (2015) 6, 267–280

Ain Shams University

Ain Shams Engineering Journal

www.elsevier.com/locate/asej
www.sciencedirect.com

MECHANICAL ENGINEERING

Natural convection heat transfer under constant heat flux wall in a nanofluid filled annulus enclosure

S.M. Seyyedi [a,*], M. Dayyan [a], Soheil Soleimani [b], E. Ghasemi [b]

[a] Department of Mechanical Engineering, Babol University of Technology, Babol, Iran
[b] Department of Mechanical Engineering, Florida International University, FL, USA

Received 25 January 2014; revised 21 August 2014; accepted 9 September 2014
Available online 18 October 2014

KEYWORDS

CVFEM;
Annulus enclosure;
Nanofluid;
Natural convection;
Constant heat flux

Abstract In this investigation, the Control Volume based Finite Element Method (CVFEM) is used to simulate the natural convection heat transfer of Cu–water nanofluid in an annulus enclosure. The Maxwell–Garnetts (MG) and Brinkman models are also employed to estimate the effect of thermal conductivity and viscosity of nanofluid. The governing parameters are the Rayleigh number, nanoparticle volume fraction and the aspect ratio (ratio of the outer radius to the inner one). Results are presented in the form of isotherms, streamlines, local and average Nusselt numbers. The results indicate that increment of the aspect ratio increases the value of average Nusselt number. Moreover, the angle of turn for the boundary condition of the inner cylinder significantly affects the values of local Nusselt number, average Nusselt number, streamlines and isotherms.

1. Introduction

Study of natural convection heat transfer in the annulus between two horizontal concentric cylinders has been the topic of interest for researchers because of the wide applications in engineering and industry such as nuclear reactor design, aircraft cabin insulation, cooling system in electronic components, solar collector–receiver, thermal storage system and vapor condenser for water distillation and food process [1,2]. The literature survey shows that there is numerous works on both experimental and numerical investigation natural convection heat transfer between two concentric circular cylinders. Kuehn and Goldstein [3] conducted an experimental and theoretical study of natural convection in concentric and eccentric horizontal cylindrical annuli. Kuehn et al. [4,5] presented experimental and numerical studies of steady-state natural convection heat transfer in horizontal concentric annuli, in which the effects of Rayleigh and Prandtl numbers and aspect ratio were parametrically explored and correlating equations, were proposed as well. The numerical and experimental analysis of natural convection from a horizontal cylinder enclosed in a rectangular cavity has been performed by Cesini et al. [6]. They investigated the effect of the cavity aspect ratio and the Rayleigh number on the isotherms and Nusselt number. Their

* Corresponding author. Tel./fax: +98 111 3234205.
E-mail addresses: mostafa_5054@yahoo.com (S.M. Seyyedi), morteza.dayyan@gmail.com (M. Dayyan), ssole016@fiu.edu (S. Soleimani), esmael.ghasemi.sahebi@gmail.com (E. Ghasemi).

Peer review under responsibility of Ain Shams University.

Production and hosting by Elsevier

http://dx.doi.org/10.1016/j.asej.2014.09.003

Nomenclature

C_p	specific heat at constant pressure
Gr_f	Grashof number
Nu_{local}	local Nusselt number
Nu_{ave}	average Nusselt number
Pr	Prandtl number ($=\upsilon/\alpha$)
T	fluid temperature
u, v	velocity components in the x-direction and y-direction
U, V	dimensionless velocity components in the X-direction and Y-direction
x, y	space coordinates
X, Y	dimensionless space coordinates
r	non-dimensional radial distance
rr	aspect ratio
k	thermal conductivity
L	gap between inner and outer boundary of the enclosure $L = r_{out} - r_{in}$
$\vec{g}$	gravitational acceleration vector
q	heat flux
Ra	Rayleigh number $(= g\beta q''(r_{out} - r_{in})^4/k_f\alpha v)$

Greek symbols

ζ	angle measured from the lower right plane
γ	angle of turn for boundary condition
α	thermal diffusivity
ϕ	volume fraction
μ	dynamic viscosity
υ	kinematic viscosity
ψ & Ψ	stream function & dimensionless stream function
Θ	dimensionless temperature
ρ	fluid density
β	thermal expansion coefficient
ε	dimensionless length of the heat source

Subscripts

c	cold
h	hot
ave	average
nf	nanofluid
f	base fluid
s	solid particles
in	inner
out	outer

results show that with increasing Rayleigh number, the average heat transfer coefficients increases. Bararnia et al. [7] studied the natural convection around a horizontal elliptic cylinder inside a square enclosure using LBM. They found that streamlines, isotherms and the number, size and formation of the cells strongly depend on the Rayleigh number and the position of inner cylinder. The forced and free convection for thermally developing and fully developed laminar airflow inside horizontal concentric annuli has been investigated experimentally by Mohammed et al. [8]. This investigation revealed that the Nusselt number is considerably greater for developing flow than the corresponding values for fully developed flow over a significant portion of the annulus. Ghaddar [9] reported the numerical results of natural convection from a uniformly heated horizontal cylinder placed in a large air-filled rectangular enclosure. He observed that flow and thermal behavior depend on heat fluxes impose on the inner cylinder within the isothermal enclosure. Hussain and Hussein [10] investigated the natural convection phenomena in a uniformly heated circular cylinder at different vertical locations immersed in a square enclosure filled with air numerically. Their result showed that the average and local Nusselt number values increase with different upward and downward locations of the inner cylinder with increasing Rayleigh number. Haldar [11] reported numerical study of combined convection through a horizontal concentric annulus using a combination of vorticity–stream function and primitive variables formulations. It was found that with increasing axial distance, the entry effect diminishes, while the buoyancy becomes stronger. Natural convection in cavities with constant flux heating at the bottom wall and isothermal cooling from the sidewalls is investigated numerically by Sharif and Mohammad [12]. They analyzed the effects aspect ratio, inclination angles, and heat source length on the convection and heat transfer process in the cavity. Their results showed that the average Nusselt number and maximum temperature change mildly with aspect ratio as well as with heat source length. Cheikh et al. [13] studied the natural convection cooling of a localized heated plate embedded symmetrically at the bottom of an air-filled square enclosure. Khanafer et al. [14] firstly conducted a numerical investigation on the heat transfer enhancement due to adding nano-particles in a differentially heated enclosure. They found that the suspended nanoparticles substantially increase the heat transfer rate at any given Grashof number. Natural convection heat transfer in an inclined enclosure filled with a water–CuO nanofluid is investigated numerically by Ghasemi and Aminossadati [15]. They found that the heat transfer rate is maximized at a specific inclination angle depending on Rayleigh number and solid volume fraction. Aminossadati and Ghasemi [16] presented the results of a numerical study on natural convection in a partially heated enclosure from below and filled with different types of nanofluids. Their results showed that the increase of solid volume fraction of nanoparticles causes the heat source maximum temperature to decrease particularly at low Rayleigh numbers. Nabavitabatabayi et al. [17] presented a numerical study on the heat transfer performance in an enclosure including nanofluids with a localized heat source. They observed that by adding nanoparticles to base liquid causes the maximum temperature decrease on account of the irregular motion of nanofluids and, more importantly, the higher energy transport rate inside the fluid. Abu-Nada et al. [18] investigated natural convection heat transfer enhancement in horizontal concentric annuli field by nanofluid. They found that for low Rayleigh numbers, nanoparticles with higher thermal conductivity cause more enhancement in heat transfer. Bararnia et al. [19] studied the natural convection in a

nanofluid filled portion cavity with a heated built in plate by LBM. The results have been obtained for different inclination angles and lengths of the inner plate. Mixed convection of a nanofluid consisting of water and SiO_2 in an inclined enclosure cavity has been studied numerically by Alinia et al. [20] using two-phase mixture model. They found that effect of inclination angle is more pronounced at higher Richardson numbers. The Control Volume based Finite Element Method (CVFEM) is new method for simulation of fluid flow and heat transfer. It uses the advantages of both finite volume and finite element methods for simulation of multi-physics problems in complex geometries [21,22]. Soleimani et al. [23] studied natural convection heat transfer in a semi-annulus enclosure filled with nanofluid using the Control Volume based Finite Element Method. They found that the angle of turn has an important effect on the streamlines, isotherms and maximum or minimum values of local Nusselt number. Ghasemi et al. [24] have been performed numerical study on Natural convection between a circular enclosure and an elliptic cylinder using Control Volume based Finite Element Method. Their results showed that streamlines, isotherms, and the number, size and formation of the cells inside the enclosure are strongly depended on these parameters which considerably enhance the heat transfer rate. Natural convection of nanofluids in an enclosure between a circular and a sinusoidal cylinder in the presence of magnetic field is studied by Sheikholeslami et al. [25]. They used Control Volume based Finite Element Method to simulate flow field and heat transfer. They found that also it is found that the average Nusselt number is an increasing function of nanoparticle volume fraction, the number of undulations and Rayleigh numbers while it is a decreasing function of Hartmann number. Sheikholeslami et al. [26–41] also have been applied CVFEM and other numerical method in order to numerical simulation of flow and heat transfer in complex flow and geometric such as Magnetohydrodynamic free convection and nanofluid.

In the present study, the effect of the Rayleigh number, nanoparticle volume fraction and aspect ratio on natural convection heat transfer in an annulus enclosure filled nanofluid has been studied numerically using the Control Volume based Finite Element Method (CVFEM).

2. Geometry definition and boundary conditions

The geometry and the mesh of the present problem are shown in Fig. 1. The outer wall is maintained at constant temperature T_c. The upper part of inner circular wall is under constant heat flux while the lower part is adiabatic. The boundary conditions for the present problem as shown in Fig. 1 are as follows:

$$\begin{cases} \Theta = 0.0 & \text{on the outer circular boundary} \\ \begin{cases} \partial\Theta/\partial n = -1.0 & \text{for } 0 < \zeta < \gamma \\ \partial\Theta/\partial n = 0.0 & \text{for } \gamma < \zeta < 360^\circ \end{cases} & \text{on the inner circular boundary} \\ \Psi = 0.0 & \text{on all solid boundaries} \end{cases} \tag{1}$$

The values of vorticity on the boundary of the enclosure can be obtained using the stream function formulation and the known velocity conditions during the iterative solution procedure.

3. Mathematical modeling and numerical procedure

3.1. Problem formulation

The flow is considered to be steady, two-dimensional, incompressible and laminar. The governing equations under

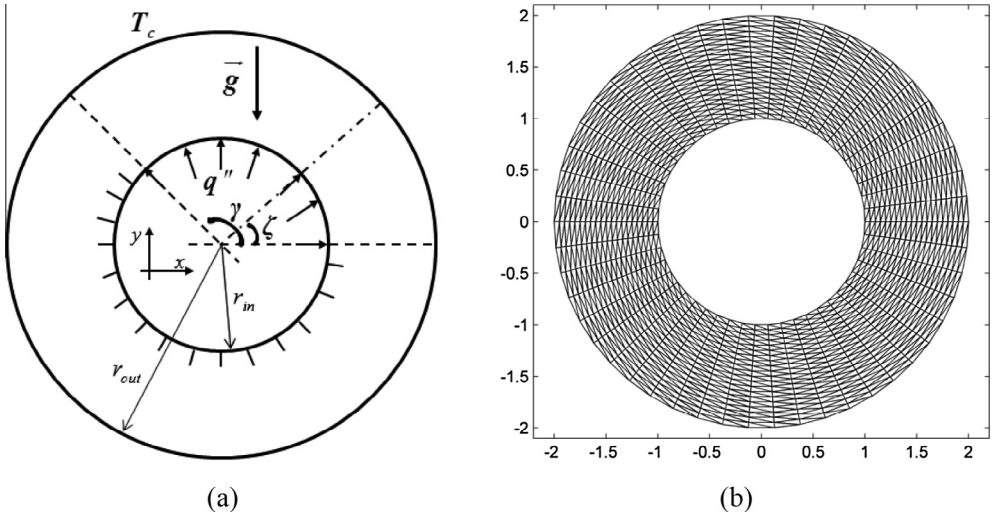

(a) (b)

Figure 1 (a) Geometry and the boundary conditions with (b) the mesh of semi-annulus enclosure considered in this work.

Table 1 Thermophysical properties of water and nanoparticles [15].

	ρ (kg/m^3)	C_p (J/kg K)	k (W/m k)	$\beta \times 10^5$ (K^{-1})
Pure water	997.1	4179	0.613	21
Copper (Cu)	8933	385	401	1.67

Table 2 Comparison of the average Nusselt number Nu_{ave} for different grid resolution at $Ra = 10^5$, $rr = 2$, $\gamma = 360°$ and $\phi = 0.06$.

Mesh size in radial direction × angular direction						
31 × 91	41 × 121	51 × 151	61 × 181	71 × 211	81 × 241	91 × 271
5.9535	5.8276	5.7572	5.7126	5.6819	5.6595	5.6595

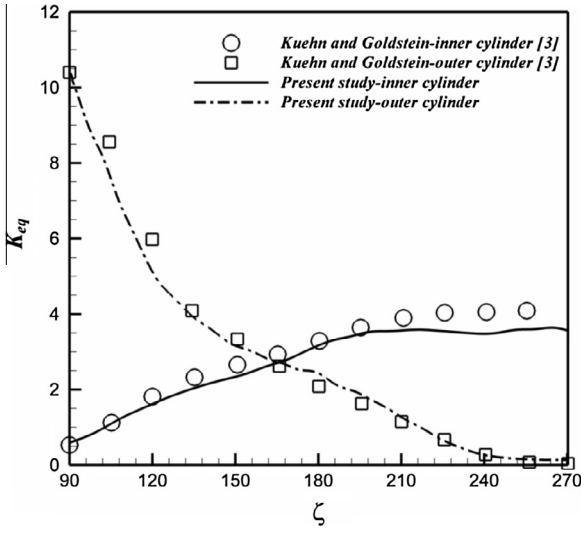

Figure 2 Comparison of the equivalent thermal conductivity on inner and outer cylinder with experimental results of Kuehn and Goldstein [3] for annulus at $Ra = 5 \times 10^4$.

Boussinesq approximation and laminar and steady state natural convection can be obtained as follows:

$$\frac{\partial u}{\partial x} + \frac{\partial v}{\partial y} = 0 \tag{2}$$

$$u\frac{\partial u}{\partial x} + v\frac{\partial u}{\partial y} = -\frac{1}{\rho_{nf}}\frac{\partial P}{\partial x} + \nu_{nf}\left(\frac{\partial^2 u}{\partial x^2} + \frac{\partial^2 u}{\partial y^2}\right) \tag{3}$$

$$u\frac{\partial v}{\partial x} + v\frac{\partial v}{\partial y} = -\frac{1}{\rho_{nf}}\frac{\partial P}{\partial y} + \nu_{nf}\left(\frac{\partial^2 v}{\partial x^2} + \frac{\partial^2 v}{\partial y^2}\right) + \beta_{nf} g(T - T_c) \tag{4}$$

Table 3 Comparison of the present solution with previous works for different Rayleigh numbers when Pr = 0.71 and $\varepsilon = 0.6$.

Gr	Present	Sharif and Mohammad [12]
10^3	3.5908	3.5558
10^4	3.7061	3.6479
10^5	5.9090	5.8641

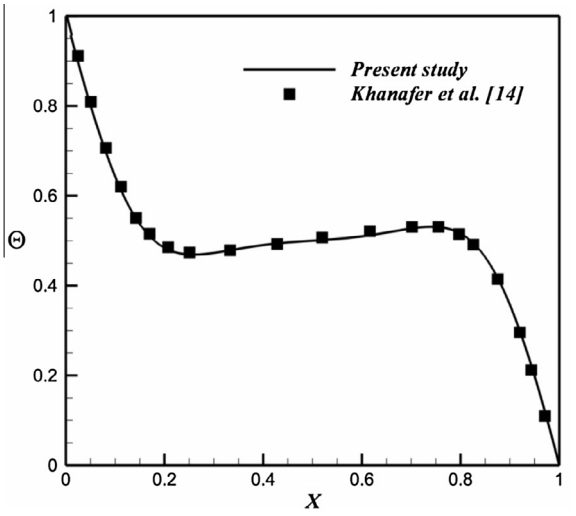

Figure 4 Comparison of the temperature on axial midline between the present results and numerical results obtained by Khanafer et al. [14] for $Gr = 10^4$, $\phi = 0.1$ and Pr = 6.2 (*Cu–Water*).

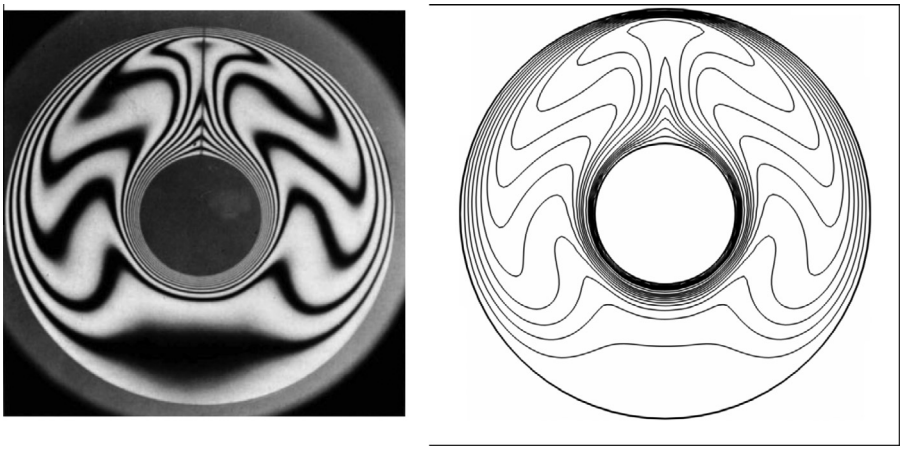

Figure 3 Comparison of the isotherms between present study and experimental study of Grigull and Hauf [42] for $Gr = 1.22 \times 10^4$.

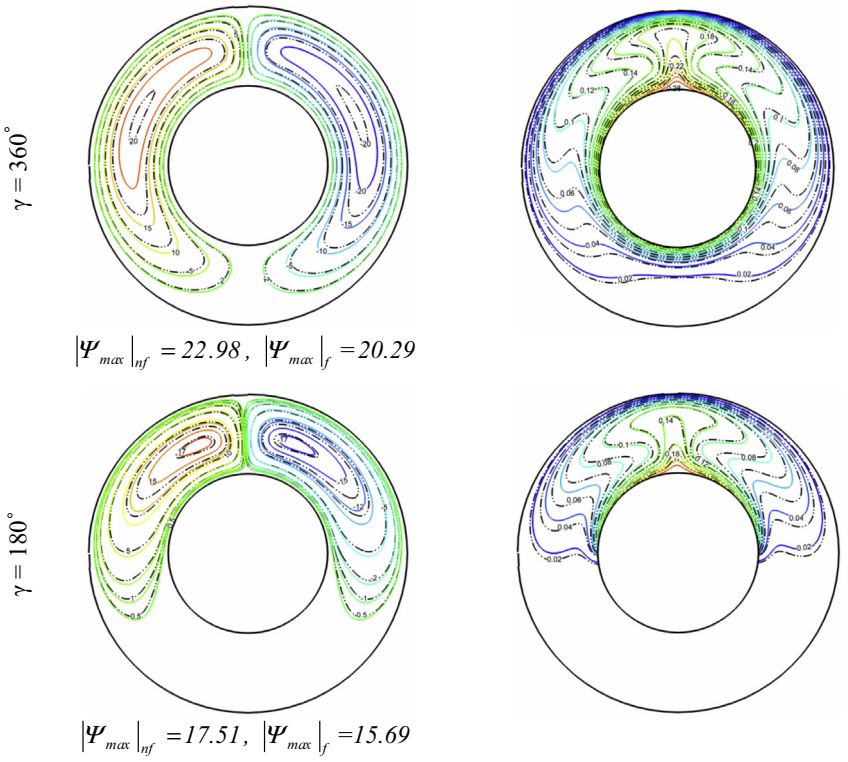

(a) $rr = 2$

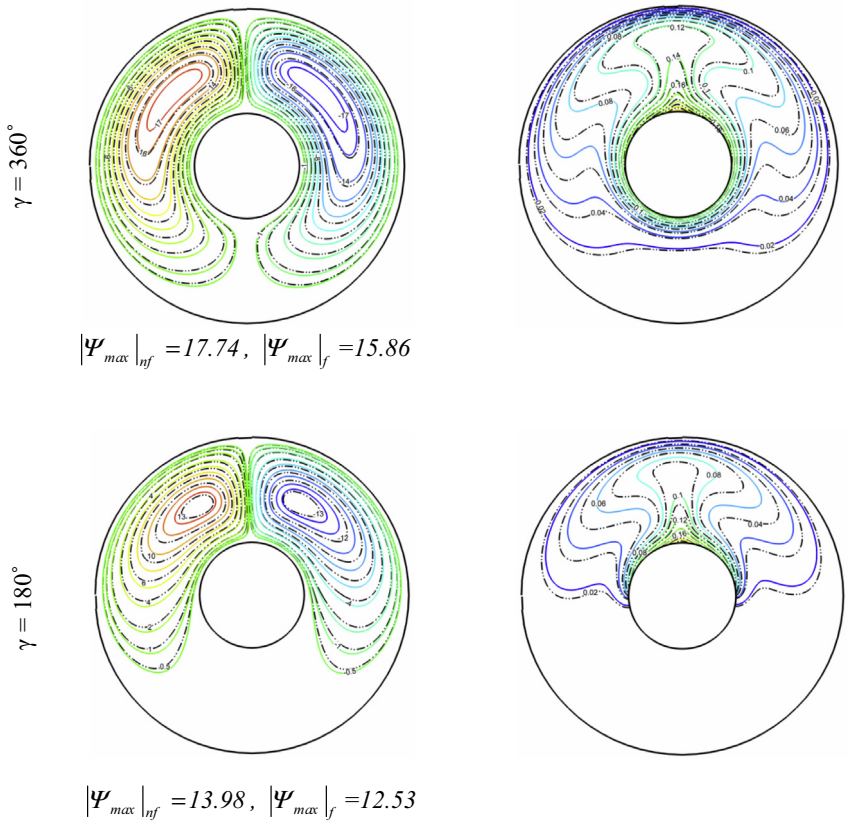

(b) $rr = 3$

Figure 5 Comparison of the streamlines (left) and isotherms (right) contours between nanofluid ($\phi = 0.06$) (—) and pure fluid ($\phi = 0$) (---) for different values of γ at $Ra = 10^5$ and Pr = 6.2.

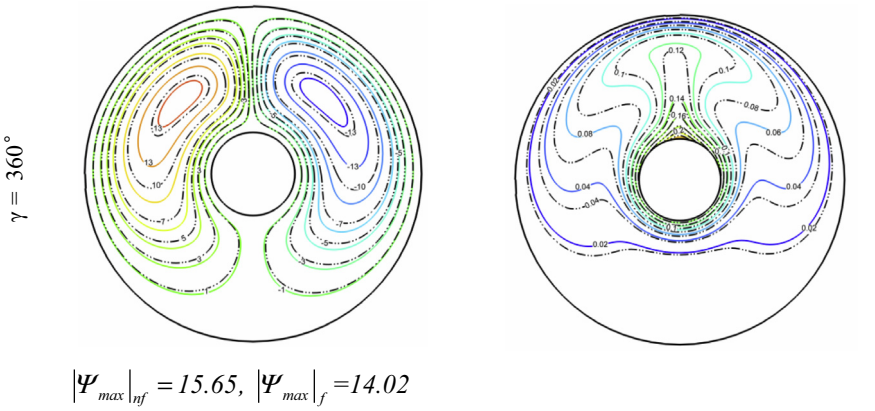

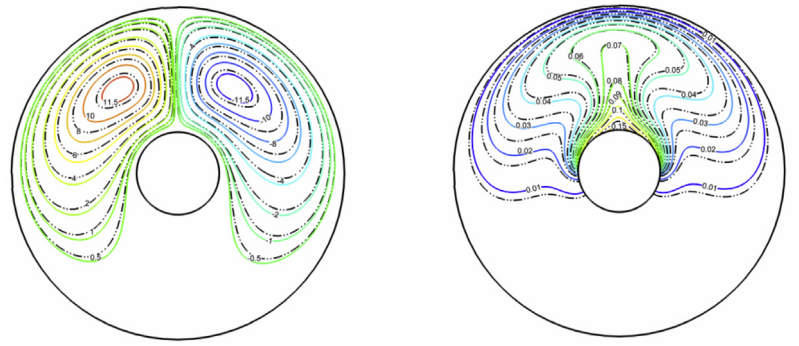

(c) $rr = 4$

Fig 5. *(continued)*

$$u\frac{\partial T}{\partial x} + v\frac{\partial T}{\partial y} = \alpha_{nf}\left(\frac{\partial^2 T}{\partial x^2} + \frac{\partial^2 T}{\partial y^2}\right) \tag{5}$$

where the effective density (ρ_{nf}) and heat capacitance $(\rho C_p)_{nf}$ of the nanofluid are defined as:

$$\rho_{nf} = \rho_f(1-\phi) + \rho_s\phi \tag{6}$$

$$(\rho C_p)_{nf} = (\rho C_p)_f\,(1-\phi) + (\rho C_p)_s\phi \tag{7}$$

where ϕ is the solid volume fraction of nanoparticles. Thermal diffusivity of the nanofluids is

$$\alpha_{nf} = \frac{k_{nf}}{(\rho C_p)_{nf}} \tag{8}$$

and the thermal expansion coefficient of the nanofluids can be determined as

$$\beta_{nf} = \beta_f(1-\phi) + \beta_s\phi \tag{9}$$

The dynamic viscosity of the nanofluids given by Brinkman [43] is

$$\mu_{nf} = \frac{\mu_f}{(1-\phi)^{2.5}} \tag{10}$$

and the effective thermal conductivity of the nanofluid can be approximated by the Maxwell–Garnetts (MG) model as [18]:

$$\frac{k_{nf}}{k_f} = \frac{k_s + 2k_f - 2\phi(k_f - k_s)}{k_s + 2k_f + \phi(k_f - k_s)} \tag{11}$$

The stream function and vorticity are defined as follows:

$$u = \frac{\partial\psi}{\partial y}, \quad v = -\frac{\partial\psi}{\partial x}, \quad \omega = \frac{\partial v}{\partial x} - \frac{\partial u}{\partial y} \tag{12}$$

The stream function satisfies the continuity Eq. (2). The vorticity equation is obtained by eliminating the pressure between the two momentum equations, i.e. by taking y-derivative of Eq. (3) and subtracting from it the x-derivative of Eq. (4). This gives:

$$\frac{\partial\psi}{\partial y}\frac{\partial\omega}{\partial x} - \frac{\partial\psi}{\partial x}\frac{\partial\omega}{\partial y} = \nu_{nf}\left(\frac{\partial^2\omega}{\partial x^2} + \frac{\partial^2\omega}{\partial y^2}\right) - \beta_{nf}g\left(\frac{\partial T}{\partial x}\right) \tag{13}$$

$$\frac{\partial\psi}{\partial y}\frac{\partial T}{\partial x} - \frac{\partial\psi}{\partial x}\frac{\partial T}{\partial y} = \alpha_{nf}\left(\frac{\partial^2 T}{\partial x^2} + \frac{\partial^2 T}{\partial y^2}\right) \tag{14}$$

$$\frac{\partial^2\psi}{\partial x^2} + \frac{\partial^2\psi}{\partial y^2} = -\omega \tag{15}$$

By introducing the following non-dimensional variables:

$$X = \frac{x}{L}, \quad Y = \frac{y}{L}, \quad \Omega = \frac{\omega L^2}{\alpha_f}, \quad \Psi = \frac{\psi}{\alpha_f},$$
$$\Theta = \frac{T - T_c}{\Delta T}, \quad \Delta T = \frac{q'' L}{k_f} \tag{16}$$

where in Eq. (16) $L = r_{out} - r_{in}$. Using the dimensionless parameters the equations now become:

$$\frac{\partial \Psi}{\partial Y}\frac{\partial \Omega}{\partial X}-\frac{\partial \Psi}{\partial X}\frac{\partial \Omega}{\partial Y}=\left[\frac{\mathrm{Pr}_f}{(1-\phi)^{2.5}\left((1-\phi)+\phi\frac{\rho_s}{\rho_f}\right)}\right]\left(\frac{\partial^2\Omega}{\partial X^2}+\frac{\partial^2\Omega}{\partial Y^2}\right)+Ra_f\mathrm{Pr}_f\left[(1-\phi)+\phi\frac{\beta_s}{\beta_f}\right]\left(\frac{\partial \Theta}{\partial X}\right) \quad (17)$$

$$\frac{\partial \Psi}{\partial Y}\frac{\partial \Theta}{\partial X}-\frac{\partial \Psi}{\partial X}\frac{\partial \Theta}{\partial Y}=\left[\frac{\frac{k_{nf}}{k_f}}{(1-\phi)+\left((1-\phi)+\phi\frac{(\rho C_p)_s}{(\rho C_p)_f}\right)}\right]\left(\frac{\partial^2\Theta}{\partial X^2}+\frac{\partial^2\Theta}{\partial Y^2}\right) \quad (18)$$

$$\frac{\partial^2 \Psi}{\partial X^2}+\frac{\partial^2 \Psi}{\partial Y^2}=-\Omega \quad (19)$$

where $Ra_f = g\beta_f L^3 q'' L/(\alpha_f \nu_f k_f)$ is the Rayleigh number for the base fluid, and $\mathrm{Pr}_f = \nu_f/\alpha_f$ is the Prandtl number for the base fluid. The fluid in the enclosure is Cu–water nanofluid and the thermo-physical properties of Cu-nano particles and based fluid are shown in Table 1 [14].

The local Nusselt number for the wall with constant heat flux is obtained for the nanofluid case using the relation:

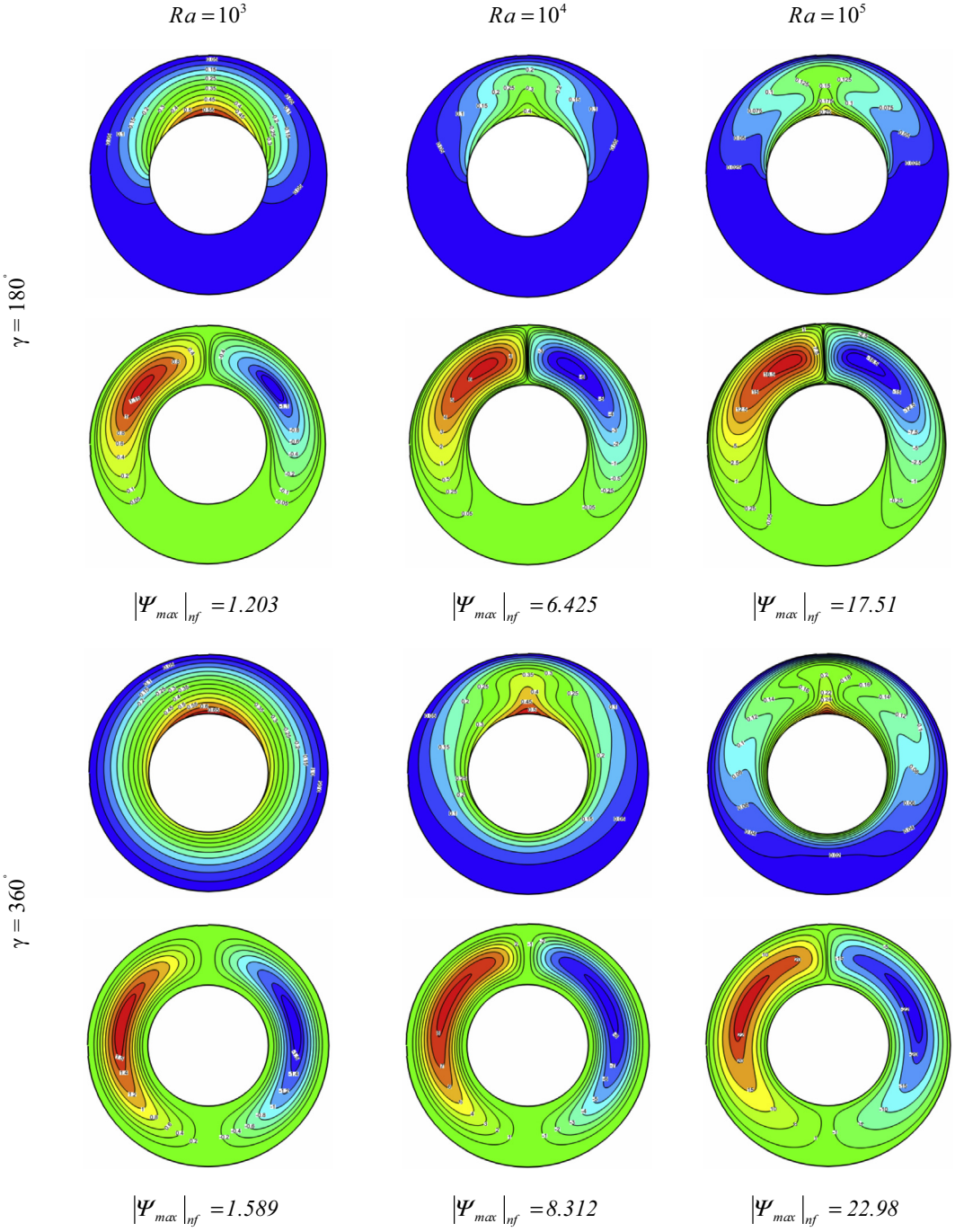

Figure 6 Comparison of the isotherms (up) and streamlines (down) contours for different values of Rayleigh numbers, γ (γ = 180° and γ = 360°), ϕ = 0.06 and at aspect ratio rr = 2.

$$Nu_{local} = \left(\frac{k_{nf}}{k_f}\right)\frac{1}{\Theta_s(\zeta)} \tag{20}$$

where Θ_s is the local dimensionless heat source temperature. The average Nusselt number is determined by integrating Nu_{local} (ζ) along the heat source:

$$Nu_{ave} = \frac{1}{\gamma}\int_0^{\gamma} Nu_{local}(\zeta)d\zeta \tag{21}$$

3.2. Physical model and numerical procedure

A FORTRAN control volume finite element method code is used in this work [44]. The building block of the discretization is the triangular element and the values of variables are approximated with linear interpolation within the elements. The control volumes are created by joining the center of each element in the support to the midpoints of the element sides that pass through the central node i which creates a close polygonal

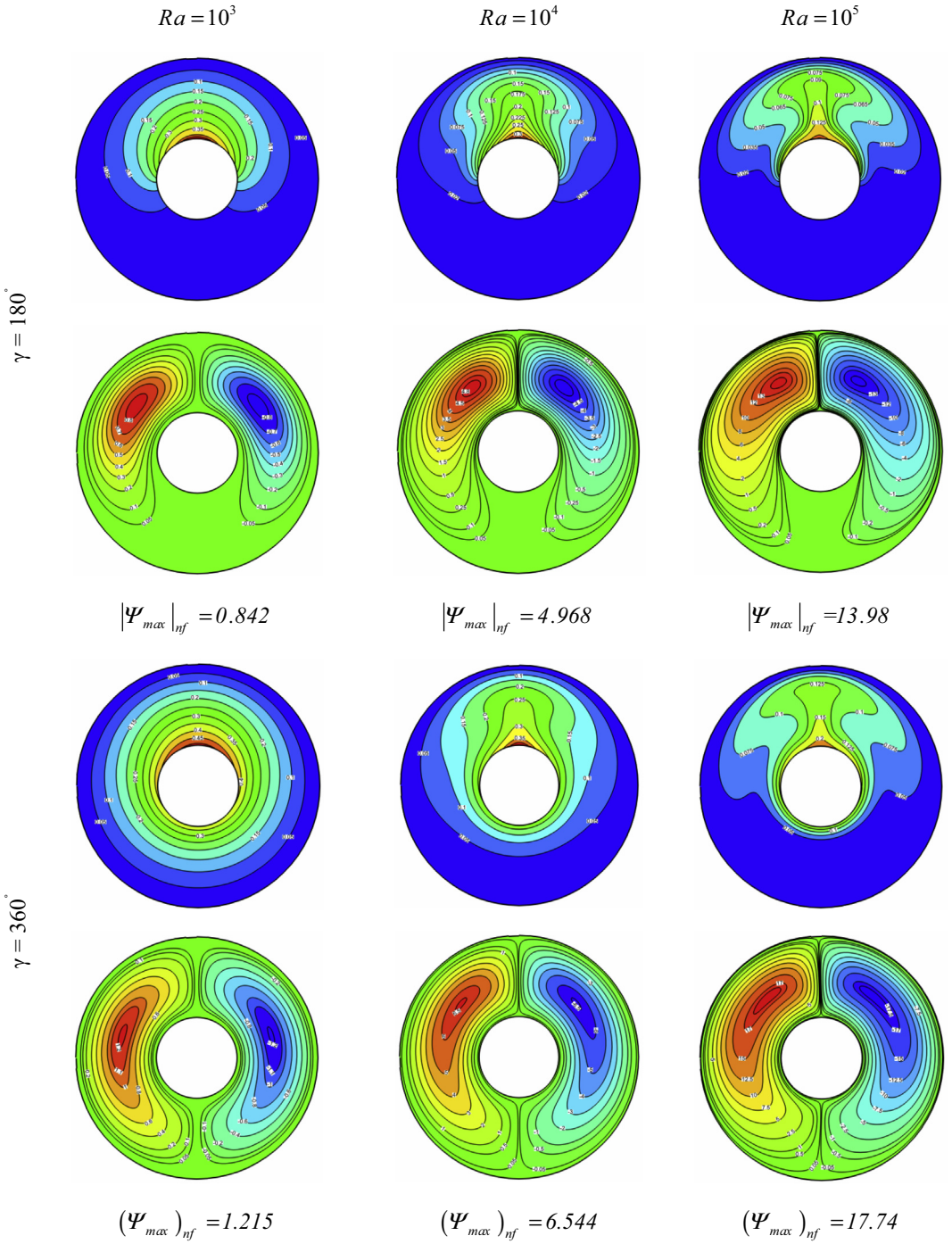

Figure 7 Comparison of the isotherms (up) and streamlines (down) contours for different values of Rayleigh numbers, γ (γ = 180° and γ = 360°) and at ϕ = 0.06, aspect ratio rr = 3.

control volume (see Fig. 1b). The set of governing equations is integrated over the Control Volume with the use of linear interpolation inside the finite element and the obtained algebretic equations are solved by the Gauss-Seidel Method.

4. Grid study and validation of the present code

To test and assess the grid independence of the solution scheme, numerical experiments are performed for eight different mesh combinations for of $Ra = 10^5$ and $\phi = 0.06$ for Cu–water nanofluid. Calculating the average Nusselt number on the inner circular wall with heat flux is used to test for grid independence in the present code. As seen in Table 2 a grid mesh of 81×241 is suitable to describe the flow and heat transfer process accurately. The convergence criterion for the termination of all computations is:

$$\max_{grid}\left|\Gamma^{m+1} - \Gamma^{m}\right| \leq 10^{-6} \tag{22}$$

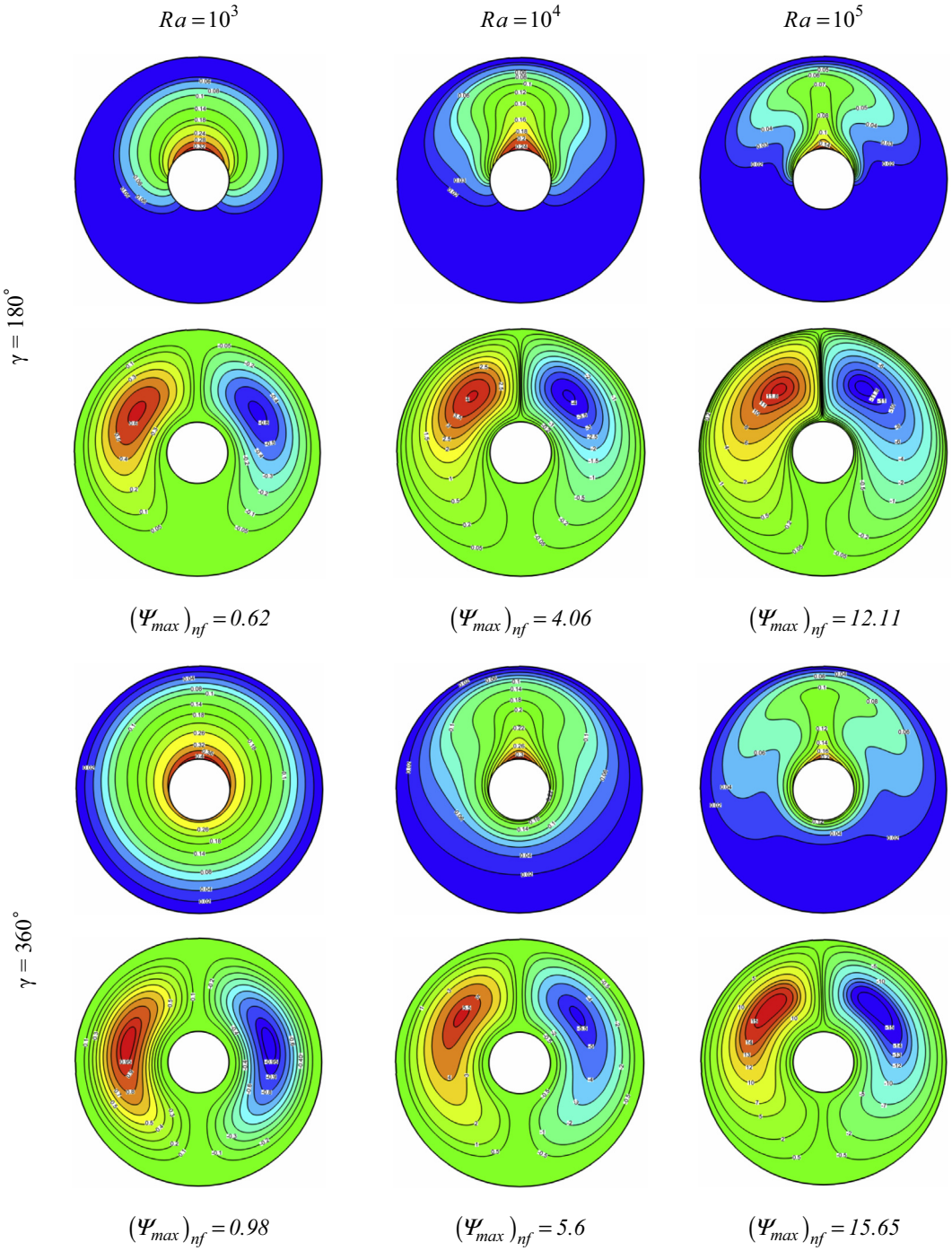

Figure 8 Comparison of the isotherms (up) and streamlines (down) contours for different values of Rayleigh numbers, γ ($\gamma = 180°$ and $\gamma = 360°$) and at $\phi = 0.06$, aspect ratio $rr = 4$.

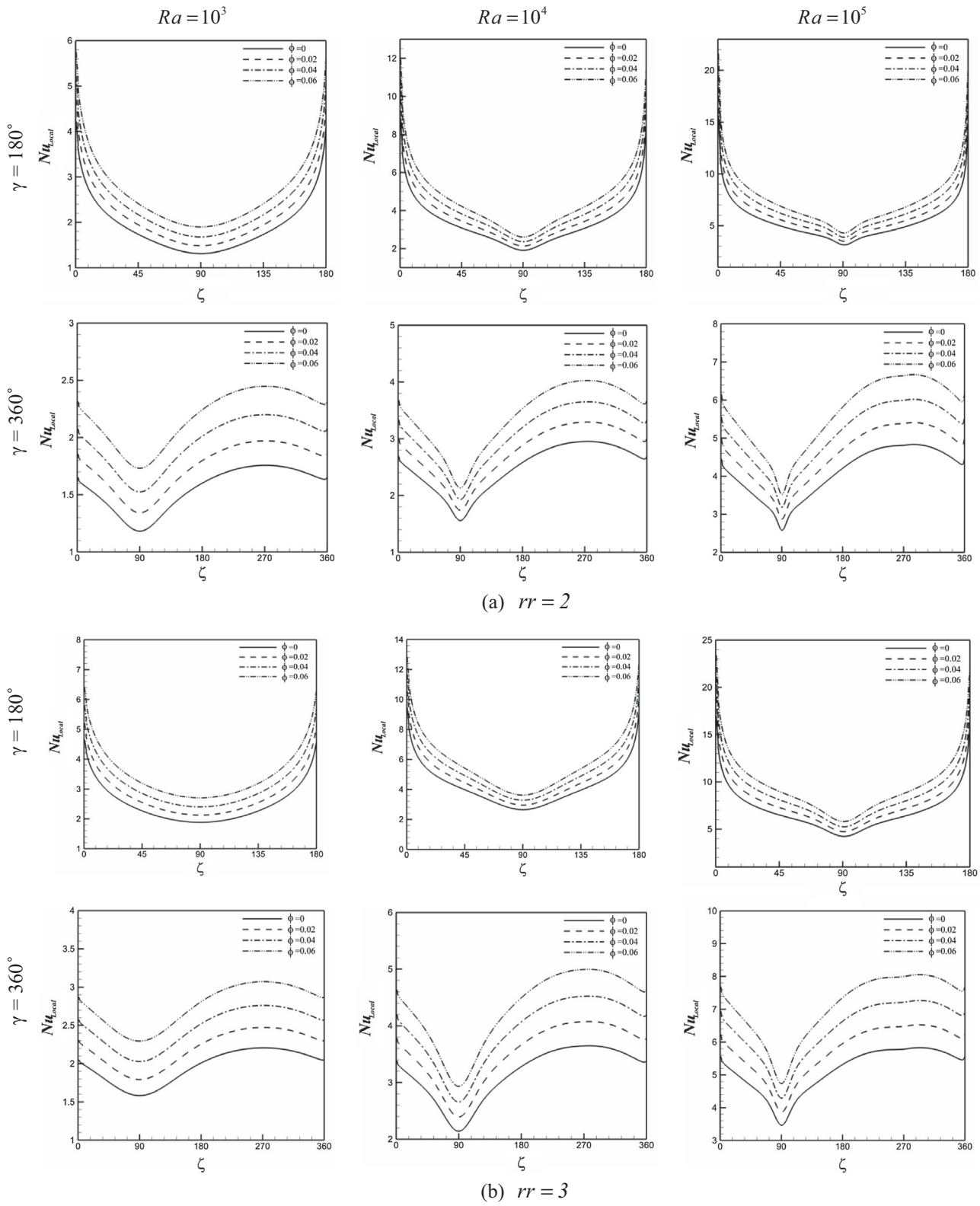

Figure 9 Profile of local Nusselt number along heat source for different of the nanoparticle volume fraction, Rayleigh number, aspect ratio and angle of turn for Cu–water nanofluids.

where m is the iteration number and Γ stands for the independent variables (Ω, Ψ, Θ).

In order to validate the numerical results of the present study they are compared with other works reported in [3,42] as seen in Figs. 2 and 3. Table 3 shows the comparison of the averaged Nusselt number versus Rayleigh number with those obtained by Sharif and Mohammad [12]. Fig. 4 illustrates an excellent agreement between the present calculations

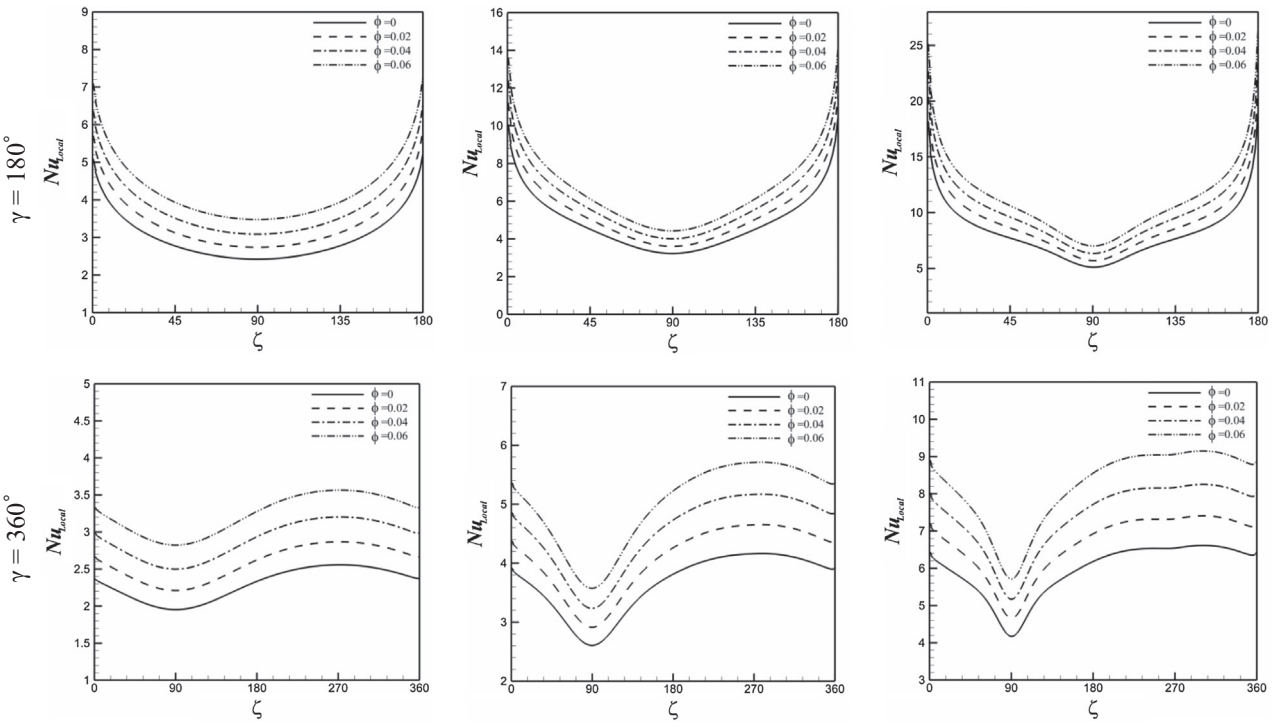

(c) $rr = 4$

Fig 9. *(continued)*

and the results of Khanafer et al. [14] for natural convection in an enclosure filled with Cu–water nanofluid. Comparison of the obtained results with the previous works shows an excellent agreement between the results.

5. Results and discussion

In the present study, natural convection heat transfer of Cu–water nanofluid in an annulus is investigated. The results obtained for various values of Rayleigh number ($Ra = 10^3, 10^4$ and 10^5), aspect ratio ($rr = 2, 3$), volume fraction of nanoparticles ($\phi = 0\%, 2\%, 4\%$ and 6%) and constant Prandtl number (Pr = 6.2).

To show the effect of nanoparticles on the streamlines and isotherms of pure fluid and nanofluid for different values of aspect ratio results are presented in Fig. 5; increasing of nanoparticles volume fraction, the velocity component increases and isotherms are expanded due to the increase in the energy transport in the fluid. Also it indicates that the effective thermal diffusion in nanofluid is greater than that in the base fluid which is due to the augmentation of effective conductivity. The sensitivity of thermal boundary layer thickness to the volume fraction of the nanoparticles is related to the increased thermal conductivity of the nanofluid. The high value of thermal diffusivity causes a drop in the temperature gradients and accordingly increases the boundary layer thickness. Thus, the absolute values of stream functions indicate that the strength of flow increases with increasing the volume fraction of nanofluid.

At $Ra = 10^3$, conduction is the dominated mechanism for heat transfer compared to the convection. The buoyancy force increases with growth of Rayleigh number which overcomes the viscous force; hence heat transfer is dominated by convection at high Rayleigh number. Fig. 6 presents the comparison of the isotherms (top) and streamline (bottom) contours for different values of Rayleigh numbers and γ ($\gamma = 180°$ and 360°) at $rr = 2$, $\phi = 6\%$. As can be seen at $Ra = 10^3$, the isotherms are uniforms and parallel to each other. As the Rayleigh number increases up to $Ra = 10^5$, the isotherms become more distorted due to the domination of convective heat transfer. In addition, the thermal boundary layer on the surface of the inner cylinder becomes thinner at higher Rayleigh number. Also a thermal plume appears at the top of the inner cylinder (heat source surface). As seen in this figure, for all cases, when γ increases, the maximum value of absolute stream function increases which indicates the domination of the convection mechanism.

The evolution of the flow and thermal fields with Rayleigh number for different values of γ ($\gamma = 180°$ and 360°) at $\phi = 6\%$ and aspect ratio of ($rr = 3, 4$) are presented in Figs. 7 and 8. Two symmetric counter-rotating rolls are formed at all Rayleigh numbers considered here. Also it is observed that for all Rayleigh number, the central vortex of the eddy is almost circular at $\gamma = 180°$ while it stretches horizontally for $\gamma = 360°$. At $\gamma = 360°$, two vortices appear at the center but when γ decrease to 180°, the center of inner vortex moves upward. As Rayleigh number increases up to 10^5, the core of the two vortices moves toward the top of inner cylinder and approaches the vertical centerline of the annulus because of the convection effect. As a result, the isotherms become more distorted above the inner cylinder. For lower Ra (10^3) the convection intensity in the annulus is very weak as obvious from the stream function values which are at least in order of magnitude smaller than those for $Ra = 10^4$ and 10^5. Thus viscous forces are more dominant than the buoyancy forces at lower

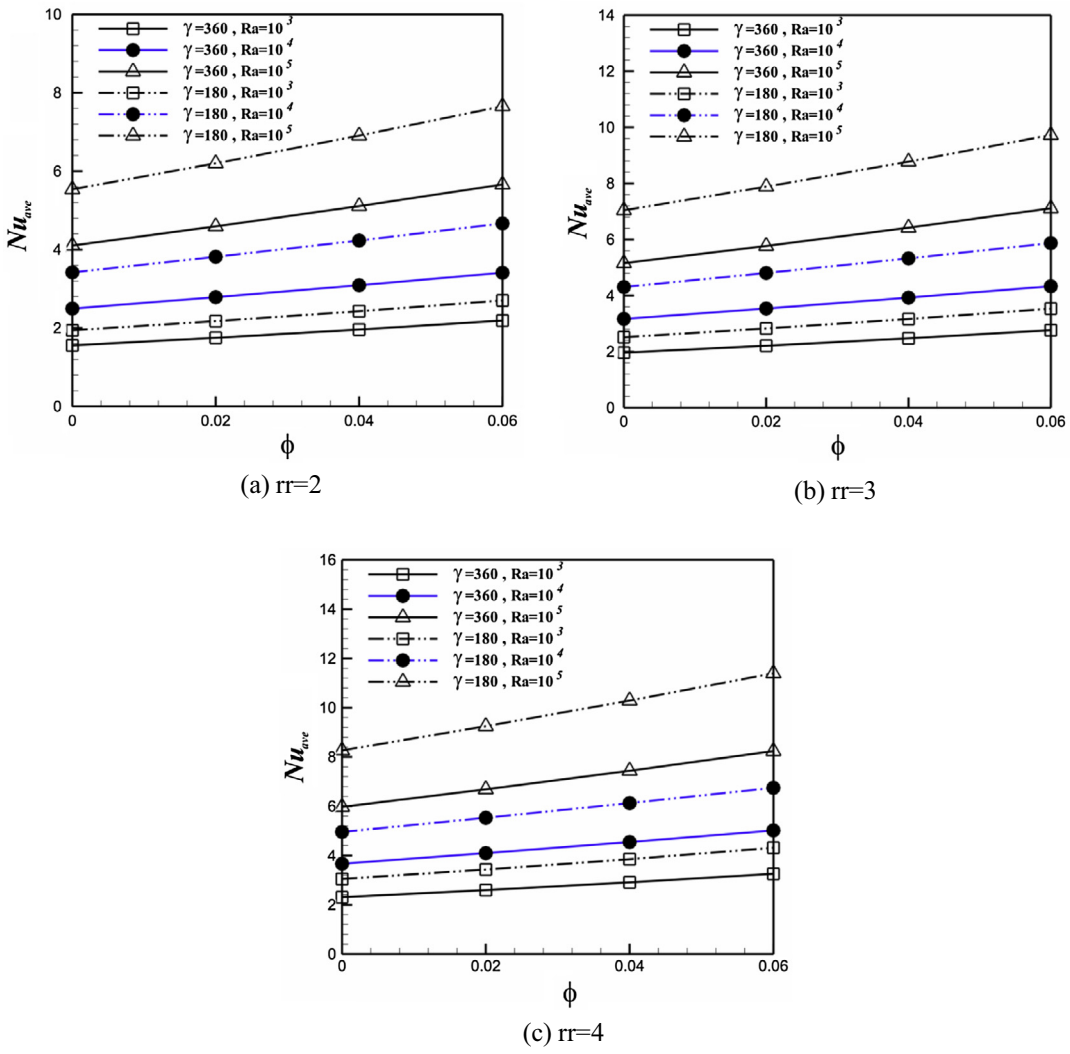

Figure 10 Variation in the average Nusselt number of heat surface with the nanoparticle volume fraction, Rayleigh number, angle of turn of boundary condition and different aspect ratio (a) $rr = 2$, (b) $rr = 3$, (c) $rr = 4$.

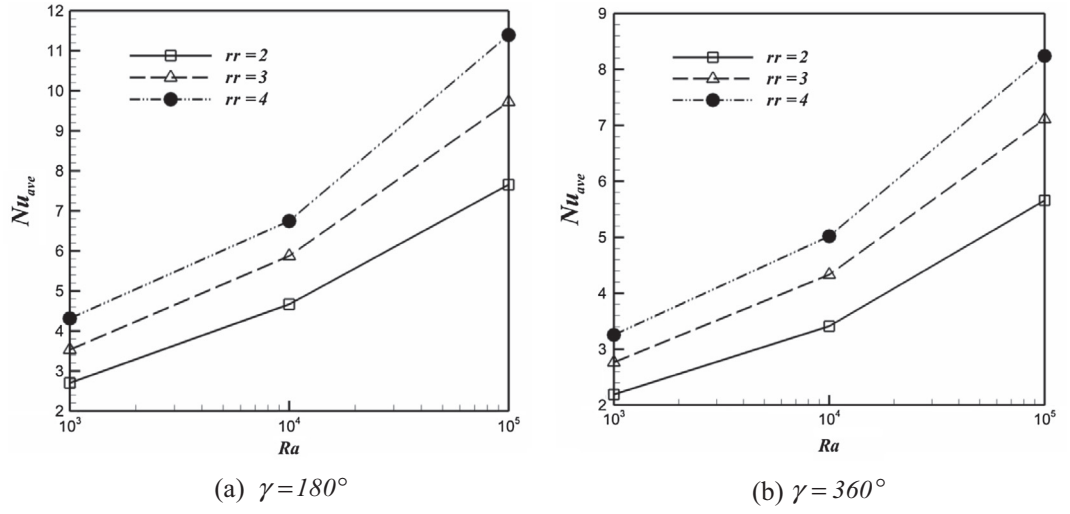

Figure 11 Comparison between the average Nusselt number of heat surface for different aspect ratio, Rayleigh number and angle of turn (a) $\gamma = 180°$, (b) $\gamma = 360°$ at $\phi = 0.06$.

Ra and diffusion is the principal mode of heat transfer. As the angle of turn (length of the heat source) increases, the value of absolute stream function increases which indicates that as γ increases, effect of the convection mechanism increases. As a result, the size of the inner circular cylinder has a great effect on streamlines and isotherms inside the circular cylinder. As shown the smaller size of inner cylinder provides the more room for flow circulation.

The local Nusselt number profile along the heated surface for different Rayleigh numbers, nanoparticle volume fractions and different angles of turn is depicted in Fig. 9. It is observed that with increasing the Rayleigh number, effect of convection increases which leads to an increase in local Nusselt number. Also for all values of γ and *rr*, the local Nusselt number increases with growth of nanoparticle volume fraction. It is to be noted that as Rayleigh number increases, the minimum and maximum values of local Nusselt number enhance. For all values of γ, the value of the local Nusselt number is minimum at $\zeta = 90°$ due to existence of thermal plumes on the surface of the inner circular wall. By increasing the aspect ratio of the annulus (*rr*), for all values of γ, volume fraction of nanoparticle and Rayleigh number and the local Nusselt number increases as a result of convective heat transfer near the heated surface of the inner cylinder. The local Nusselt number profile is almost symmetric to the vertical centerline and the minimum value of Nu_{local} is obtained at $\zeta = 90°$ where the isotherms are coarsest by the occurrence of the plume. At $\gamma = 360°$, the profile of local Nusselt number at $rr = 2, 3$ and 3 is the same but the value of Nusselt number at $rr = 4$ is greater than that for $rr = 2$ and 3.

Variations in the average Nusselt number on the heat source as a function of the angle of turn and nanoparticle volume fraction for different Rayleigh numbers and aspect ratio ($rr = 2$, 3 and 4) are presented in Fig. 10. As can be seen from the figure, for all values of *rr* and γ, the average Nusselt number increases with increase of nanoparticle volume fraction and Rayleigh number. Also it can be observed that, the variation in average Nusselt number with respect to γ is small at $Ra = 10^3$. At $Ra = 10^4$, the variation in average Nusselt number is more noticeable than $Ra = 10^3$. For all value of Rayleigh number, the average Nusselt number at $\gamma = 180°$ is greater than that of $\gamma = 360°$. As seen in Fig. 10, with increase of aspect ratio from 2 to 3 and 4, the average Nusselt number increases for all values of Rayleigh number. Also it can be found that the effect of nanoparticles is more pronounced at low Rayleigh number than that at high Rayleigh number because of the greater heat transfer enhancement rate. This observation can be explained by noting that at low Rayleigh number the heat transfer is dominant by conduction. Therefore, the addition of high thermal conductivity nanoparticles will increase the conduction and make the heat transfer enhancement more effective. Fig. 11 shows the comparison between the average Nusselt number of hot surface for different aspect ratio, Rayleigh number and angle of turn at $\phi = 0.06$. These figures show that when the aspect ratio enhances, the average Nusselt number increases.

6. Conclusions

This study investigates the natural convection heat transfer natural convection heat transfer of Cu–water nanofluid in an annulus. The upper part of inner circular wall is under the constant heat flux while the lower part is adiabatic and outer circular cylinder has constant cold temperature. The Control Volume based Finite Element Method (CVFEM) was used for flow and thermal fields. The numerical results are obtained for different values of volume fraction of the nanoparticles, Rayleigh numbers, angle of turn for boundary condition of the inner cylinder and aspect ratios. The important results are presented as follows:

- The average Nusselt number is an increasing function of Rayleigh numbers.
- The increase of volume fraction of the nanoparticles causes a greater average Nusselt number particularly at high Rayleigh numbers where the convection is the main heat transfer mechanism.
- The increase of aspect ratio increases the value of average Nusselt number.
- The minimum values of local Nusselt number is corresponding to existence of thermal plumes on the top surface of the inner circular wall of the enclosure ($\gamma_{min} = 90°$).
- As the angle of turn for boundary condition of the inner cylinder increases, the value of averaged Nusselt number on the heat source reduces.

References

[1] Glakpe EK, Watkins CB, Cannon JN. Constant heat-flux solutions for natural convection between concentric and eccentric horizontal cylinders. Numer Heat Transfer 1986;10:279–95.

[2] Kim BS, Lee DS, Ha MY, Yoon HS. A numerical study of natural convection in a square enclosure with a circular cylinder at different vertical locations. Int Heat Mass Transfer 2008;51:1888–906.

[3] Kuehn T, Goldstein R. An experimental and theoretical study of natural convection in the annulus between horizontal concentric cylinders. J Fluid Mech 1976;74:695–719.

[4] Kuehn T, Goldstein R. A parametric study of Prandtl number and diameter ratio effects on natural convection heat transfer in horizontal cylindrical annuli. J Heat Transfer 1978;102:768–70.

[5] Kuehn TH, Goldstein RJ. Correlating equations for natural convection heat transfer between horizontal circular cylinders. Int J Heat Mass Transfer 1976;19:1127–34.

[6] Cesini G, Paroncini M, Cortellab G, Manzan M. Natural convection from a horizontal cylinder in a rectangular cavity, convection in a horizontal annulus driven by inner heat generating solid cylinder. Int J Heat Mass Transfer 1999;42:1801–11.

[7] Bararnia H, Soleimani Soheil, Ganji DD. Lattice Boltzmann simulation of natural convection around a horizontal elliptic cylinder inside a square enclosure. Int Commun Heat Mass Transfer 2011;38:1436–42.

[8] Mohammed HA, Campo Antonio, Saidur R. Experimental study of forced and free convective heat transfer in the thermal entry region of horizontal concentric annuli. Int Commun Heat Mass Transfer 2010;37:739–47.

[9] Ghaddar NK. Natural convection heat transfer between a uniformly heated cylindrical element and its rectangular enclosure. Int J Heat Mass Transfer 1992;35:2327–34.

[10] Hussain SH, Hussein AK. Numerical investigation of natural convection phenomena in a uniformly heated circular cylinder immersed in square enclosure filled with air at different vertical locations. Int Commun Heat Mass Transfer 2010;37:1115–26.

[11] Haldar SC. Combined convection in developing flow through a horizontal concentric annulus. Numer Heat Transfer A 1998;34(6):673–85.

[12] Sharif MAR, Mohammad TR. Natural convection in cavities with constant flux heating at the bottom wall and isothermal cooling from the sidewalls. Int J Therm Sci 2005;44:865–78.
[13] Cheikh NB, Beya BB, Lili T. Influence of thermal boundary conditions on natural convection in a square enclosure partially heated from below. Int Commun Heat Mass Transfer 2007;34:369–79.
[14] Khanafer K, Vafai K, Lightstone M. Buoyancy-driven heat transfer enhancement in a two-dimensional enclosure utilizing nanofluids. Int J Heat Mass Transfer 2003;46:3639–53.
[15] Ghasemi B, Aminossadati SM. Natural convection heat transfer in an inclined enclosure filled with a water–CuO nanofluid. Numer Heat Transfer A Appl 2009;55:807–23.
[16] Aminossadati SM, Ghasemi B. Natural convection cooling of a localised heat source at the bottom of a nanofluid-filled enclosure. Eur J Mech B/Fluids 2009;28:630–40.
[17] Nabavitabatabayi Mohammad reza, Shirani Ebrahim, Rahimian Mohammad Hassan. Investigation of heat transfer enhancement in an enclosure filled with nanofluids using multiple relaxation time Lattice Boltzmann modeling. Int Commun Heat Mass Transfer 2011;38:128–38.
[18] Abu-Nada E, Masoud Z, Hijazi A. Natural convection heat transfer enhancement in horizontal concentric annuli using nanofluids. Int Commun Heat Mass Transfer 2008;35:657–65.
[19] Bararnia H, Hooman K, Ganji DD. Natural convection in a nanofluid filled portion cavity; the Lattice-Boltzmann method. Numer Heat Transfer Part A 2011;59:487–502.
[20] Alinia M, Ganji DD, Gorji-Bandpy M. Numerical study of mixed convection in an inclined two sided lid driven cavity filled with nanofluid using two-phase mixture model. Int Commun Heat Mass Transfer 2011;38:1428–35.
[21] Baliga BR. Control-volume finite element methods for fluid flow and heat transfer. In: Minkowycz WJ, Sparrow EM, editors. Advances in numerical heat transfer, vol. 1. New York: Taylor & Francis; 1996. p. 97–136.
[22] Baliga BR, Patankar SV. A control volume finite-element method for two-dimensional fluid flow and heat transfer. Numer Heat Transfer 1983;6:245–61.
[23] Soleimani Soheil, Sheikholeslami M, Ganji DD, Gorji-Bandpay M. Natural convection heat transfer in a nanofluid filled semi-annulus enclosure. Int Commun Heat Mass Transfer 2012;39:565–74.
[24] Ghasemi E, Soleimani Soheil, Bararnia H. Natural convection between a circular enclosure and an elliptic cylinder using Control Volume based Finite Element Method. Int Commun Heat Mass Transfer 2012;39:1035–44.
[25] Sheikholeslami M, Gorji-Bandpy M, Ganji DD, Soleimani Soheil, Seyyedi SM. Natural convection of nanofluids in an enclosure between a circular and a sinusoidal cylinder in the presence of magnetic field. Int Commun Heat Mass Transfer 2012;39:1435–43.
[26] Sheikholeslami M, Gorji-Bandpy M, Ganji DD, Rana P, Soleimani Soheil. Magnetohydrodynamic free convection of Al_2O_3–water nanofluid considering thermophoresis and Brownian motion effects. Comput Fluids 2014;94:147–60.
[27] Sheikholeslami M, Gorji-Bandpy M, Ganji DD, Soleimani Soheil. Thermal management for free convection of nanofluid using two phase model. J Mol Liq 2014;194:179–87.
[28] Sheikholeslami M, Gorji-Bandpy M, Ganji DD, Soleimani Soheil. Magnetic field effect on nanofluid flow and heat transfer using KKL model. J Taiwan Inst Chem Eng 2014;45:795–807.
[29] Sheikholeslami M, Gorji-Bandpy M, Soleimani Soheil. Two phase simulation of nanofluid flow and heat transfer using heatline analysis. Int Commun Heat Mass Transfer 2013;47:73–81.
[30] Sheikholeslami M, Gorji-Bandpy M, Ellahi R, Hassan Mohsan, Soleimani Soheil. Effects of MHD on Cu–water nanofluid flow and heat transfer by means of CVFEM. J Magn Magn Mater 2014;349:88–200.
[31] Sheikholeslami M, Gorji-Bandpy M, Ganji DD, Soleimani Soheil. Natural convection heat transfer in a cavity with sinusoidal wall filled with CuO–water nanofluid in presence of magnetic field. J Taiwan Inst Chem Eng 2014;45:40–9.
[32] Sheikholeslami M, Gorji-Bandpy M, Ganji DD, Soleimani Soheil. Heat flux boundary condition for nanofluid filled enclosure in presence of magnetic field. J Mol Liq 2014;193:174–84.
[33] Sheikholeslami M, Gorji-Bandpy M, Ganji DD. Magnetic field effects on natural convection around a horizontal circular cylinder inside a square enclosure filled with nanofluid. Int Commun Heat Mass Transfer 2012;39:978–86.
[34] Sheikholeslami M, Gorji-Bandpy M, Ganji DD. MHD free convection in an eccentric semi-annulus filled with nanofluid. J Taiwan Inst Chem Eng 2014;45:1204–16.
[35] Sheikholeslami M, Gorji-Bandpy M. Free convection of ferrofluid in a cavity heated from below in the presence of an external magnetic field. Powder Technol 2014;256:490–8.
[36] Sheikholeslami M, Gorji-Bandpy M, Ganji DD. Lattice Boltzmann method for MHD natural convection heat transfer using nanofluid. Powder Technol 2014;254:82–93.
[37] Sheikholeslami M, Gorji-Bandpy M, Ganji DD. Numerical investigation of MHD effects on Al_2O_3–water nanofluid flow and heat transfer in a semi-annulus enclosure using LBM. Energy 2013;60:501–10.
[38] Sheikholeslami M, Gorji-Bandpy M, Seyyedi SM, Ganji DD, Rokni Houman B, Soleimani Soheil. Application of LBM in simulation of natural convection in a nanofluid filled square cavity with curve boundaries. Powder Technol 2013;247:87–94.
[39] Sheikholeslami M, Gorji-Bandpy M, Ganji DD. Natural convection in a nanofluid filled concentric annulus between an outer square cylinder and an inner elliptic cylinder. Sci Iranica Trans B Mech Eng 2013;20(4):1241–53.
[40] Sheikholeslami M, Gorji-Bandpy M, Domairry G. Free convection of nanofluid filled enclosure using Lattice Boltzmann method (LBM). Appl Math Mech 2013;34(7):1–15.
[41] Sheikholeslami M, Gorji-Bandpy M, Domairry G. Free convection of nanofluid filled enclosure magnetic field effects on natural convection flow of a nanofluid in a horizontal cylindrical annulus using Lattice Boltzmann method. Int J Therm Sci 2013;64:240–50.
[42] Grigull U, Hauf W. Natural convection in horizontal cylindrical annuli; 1966.
[43] Wang XQ, Mujumdar AS. Heat transfer characteristics of nanofluids: a review. Int J Therm Sci 2007;46(1):1–19.
[44] Sheikholeslami M, Gorji-Bandpy M, Ganji DD, Soleimani Soheil. Effect of a magnetic field on natural convection in an inclined half-annulus enclosure filled with Cu–water nanofluid using CVFEM. Adv Powder Technol 2013;24:980–91.

Seyyed Mostafa Seyyedi Taji (S.M. Seyyedi) received his B.Sc. degree from school of Mechanical Engineering in Thermo-fluid subfield at Mazandaran University and his M.Sc. degree in Energy Conversion subfield from Department of Mechanical Engineering at Babol University of Technology. His main research interests are Computational Fluid Dynamics and Computational physics, Mesoscopic modeling of fluid flow using LBM and Multiphase flow.